Open Access Online Journal on Astronomy and Astrophysics

Acta Astrophysica Taurica

www.astrophysicatauricum.org

Acta Astrophys. Tau. 5(4), 11–16 (2024)

Observation of solar flare SOL 2015–10–01 and calculation of its radiation within the model of superposition of heated layers

Yu.A. Kupryakov[1,2], K.V. Bychkov[2], O.M. Belova[2], A.B. Gorshkov[2], P. Kotrč[1]

[1] Astronomical Institute ASCR, Fričova 298, Ondřejov 251 65, Czech Republic
e-mail: kupry@asu.cas.cz
[2] Sternberg Astronomical Institute, Moscow State University, Universitetsky pr. 13, Moscow 119234, Russia

Received 30 November 2022

ABSTRACT

The purpose of the work is to study the behavior of intensity curves emission in the Hα, Hβ, D3, H Ca II, and Ca IR 8542 Å lines in the process of development of the flare and compare the results with calculated values. Observations were carried out with the horizontal solar telescope HSFA-2 (Ondřejov Observatory) using CCD arrays. For processing we selected the 2015–10–01 flare of class M 4.5 in the NOAA active region 12422 for which the absolute values of the fluxes in spectral lines were determined. It is shown that the model of heating of the chromospheric gas by the flow of magnetohydrodynamic waves from the convective zone and its ionization and excitation by the flow of suprathermal particles from the corona satisfies the observations. Calculations are performed in the lines of hydrogen, the Ca II ion, and the helium atom, taking into account the main processes determining the radiation of gas that is opaque in spectral lines. It is shown that at the onset of the flare, the emission in the Ca II lines comes from a cold region, with a temperature of about 5400 K, in the sunspot penumbra. The flat decrement of the Balmer series coupled with a large flux in the calcium lines indicates the inhomogeneity of the radiating region along the vertical. The emission in the helium D3 line is largely due to suprathermal particles.

Key words: solar flare, chromosphere, spectral lines, homogeneous gas layer model

1 Introduction

The study of spectral line behavior during a flare is of great interest. For example, the formation and temporal evolution of Ca II lines remains a mystery, including why they respond slowly to flares compared to Balmer series lines. This may be related to the formation of a time-dependent nonthermal electron model of heating of the impulsive phase in the lower chromosphere (Abbett, Hawley, 1999; Allred et al., 2006), or this may be associated with a hotter, higher region in the flaring chromosphere (Schmidt et al., 2012). Models of backwarming by coronal X-rays have shown that a relatively large amount of Ca II emission occurs for a range of heights in the flare chromosphere with T = 5000–7600 K (Hawley, Fisher, 1992). A temporal scenario considered a process in which hot chromospheric loops cool down to the temperature of formation of Ca II lines (Houdebine, 2003; Crespo-Chacón et al., 2006). In this work, we consider emission in spectral lines and the X-ray range within the framework of a model of the joint action of MHD waves and a flux of suprathermal particles. MHD waves carry heat fluxes from below, from the subphotospheric layers, while suprathermal particles ionize and excite the gas as they move down from the corona.

2 Observations and data reduction

We aim to study the behavior of radiation intensity curves in the Hα, Hβ, D3, H Ca II and Ca IR 8542 Å lines during the development of a flare and compare the results with calculated values. To determine possible luminescence mechanisms in lines, the radiation flux in each line was calculated. We performed calculations within the framework of a model of a set of homogeneous gas layers, selecting their parameters in such a way that the theoretical radiation fluxes turn out to be close to the observed ones. Observations were carried out with the horizontal solar telescope HSFA-2 using CCD matrices (Kotrč, 2009). We selected the 2015–10–01 flare of class M 4.5 in the NOAA AR 12422 [S18W66]. Figure 1a shows a course of X-ray emission during the flare; vertical lines correspond to the moments of data processing. Figure 1b shows an image of the active region in the 171 Å line (SDO data) obtained by the subtraction method. Hot loops are clearly visible; their position and structure did not change during the flare, which indicates a strong magnetic field. An image of the chromosphere in the Hα line at the spectrograph slit (SJ) and spectra are shown in Fig. 2. After data reduction, line profiles were obtained in the active and quiet regions of the chromosphere (Figs. 2 and 3). By integrating the difference between them (areas shaded in gray in Fig. 3) over the

Table 1. Values of integral fluxes in lines in erg/cm^2/s and their ratio at the following time moments: (I) 13:07:54, (II) 13:08:34, and (III) 13:10:38 UT.

UT, hms	Hα	Hβ	α/β	H Ca II 3968	IR Ca II 8542	R/I	D_3HeI 5876
13:07:54	$1.13\,10^7$	$7.81\,10^6$	1.45	$1.11\,10^7$	$4.77\,10^6$	2.33	$3.80\,10^5$
13:08:34	$2.84\,10^7$	$1.89\,10^7$	1.50	$1.82\,10^7$	$1.27\,10^7$	1.43	$5.95\,10^5$
13:10:38	$3.13\,10^7$	$2.57\,10^7$	1.22	$2.38\,10^7$	$1.32\,10^7$	1.80	$1.26\,10^6$

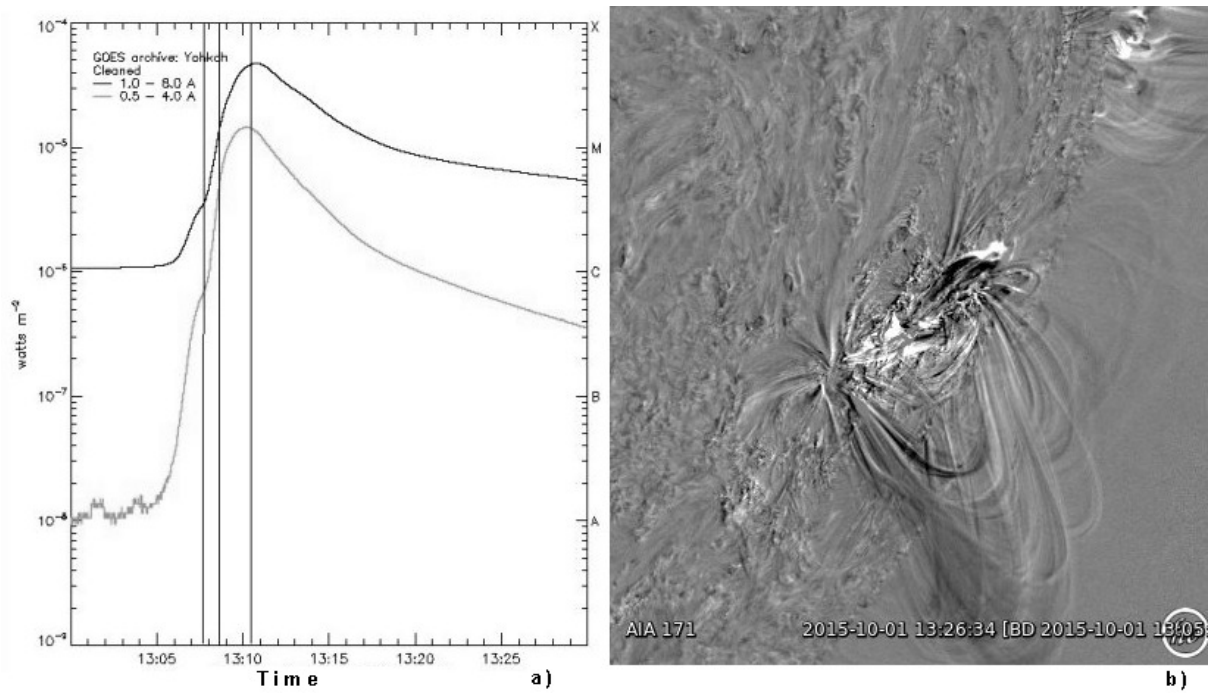

Fig. 1. a) Change in the X-ray flux during the flare (GOES 15 data); the values selected for processing are marked. b) Structure of the flare in the 171 Å line (the image was obtained by subtracting the frame at 13:26:34 UT from the image at 13:05:30 UT). Chromospheric loops are clearly visible in the image.

spectrum and, assuming the isotropy of the radiation field at each point, over the solid angle, the values of radiation fluxes were determined (Table 1).

3 Model and calculation method

In the proposed model, the sporadic enhancement of radiation in the spectral lines of hydrogen, helium and metals occurs due to an increase in the thermal flux from the subphotospheric layers, as well as by ionization and excitation of ions and atoms by a flux of suprathermal particles. The upward thermal flux is carried by a triad of magnetohydrodynamic waves: Alfvén, fast, and slow acoustic waves. Alfvén waves, due to a weak damping, can propagate over long distances up to the coronal layers. Gas heating occurs mainly during the damping of slow acoustic waves, whose phase velocity is close to the thermal velocity. The conversion of Alfvén waves into slow sound is implemented through the scattering of fast magnetosonic waves on plasma inhomogeneities. The downward flux of energetic particles from the corona, manifesting itself by X-ray emission, according to modern concepts, is formed after the release of energy as a result of the reconnection of magnetic field lines.

We performed calculations within the framework of the model with a set of homogeneous gas layers, selecting their parameters in such a way that the theoretical radiation fluxes turn out to be close to the observed ones. The magnitude of heating by MHD waves is set by the choice of the gas temperature T_e. For the convenience of calculations, we describe suprathermal particles as a gas with a certain temperature T_f and energy flux density J. We set the value of T_f equal to 15 keV. We took the radiation field to be blackbody; its temperature is denoted by T_b. According to the calculation results presented in the next section, we set the value of T_b equal to 5400 K, which is the temperature of the sunspot penumbra. The importance of taking into account photospheric radiation is shown in Grinin, Katysheva (1980), Bychkov, Morchenko (2011), Belova, Bychkov (2018).

The power of linear radiation is determined by the population of excited levels and the effective probability of pho-

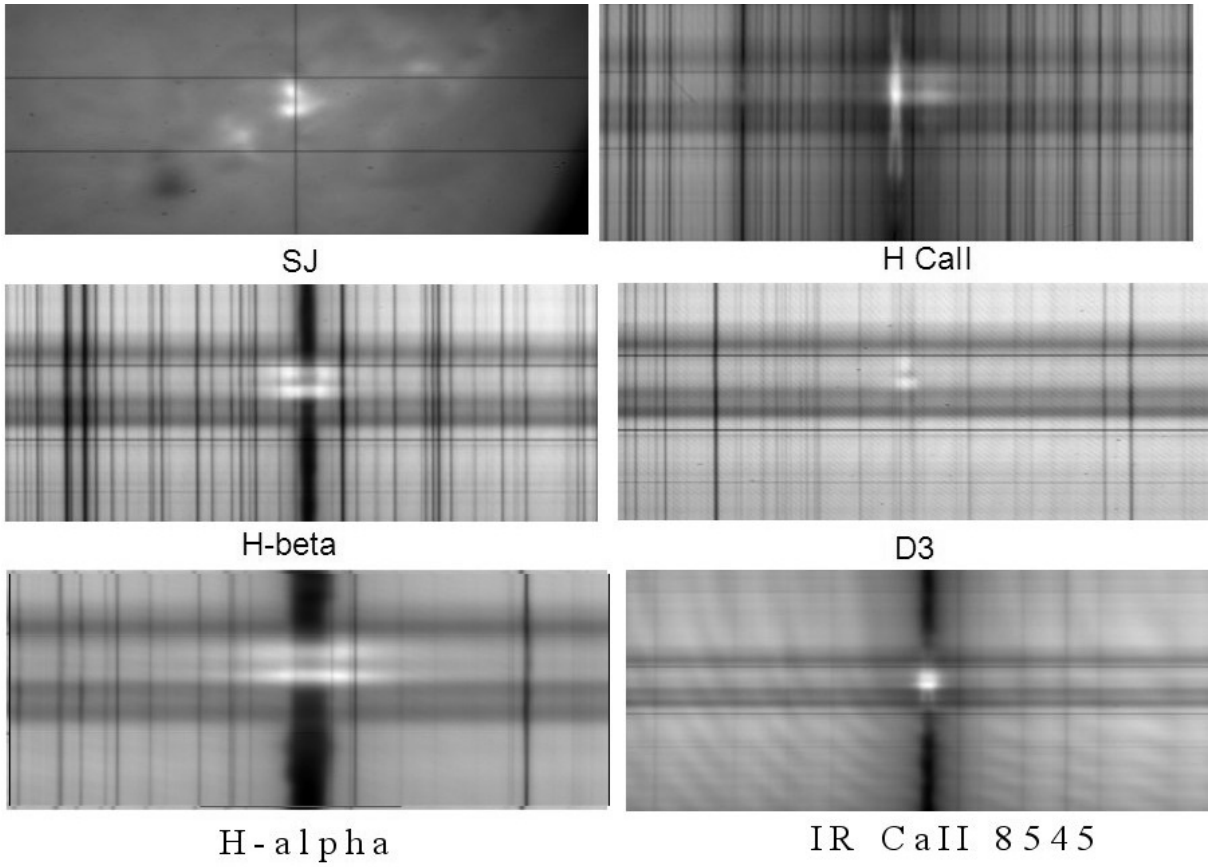

Fig. 2. Image of the chromosphere at the slit in the Hα line (SJ) and reduced spectra.

ton escape, taking into account scattering. We determine the population of discrete levels and the state of ionization by solving the balance equations. The hydrogen model includes 12 discrete levels and a continuum; oscillator strengths and radiative transition rates are taken from Johnson (1972), the photoionization cross-section was used in the Kramers approximation. The helium model includes 29 discrete levels (up to $n = 5$) and a continuum; level energies and oscillator strengths are taken from NIST (National Institute of Standards and Technology). The Ca II ion model includes five discrete levels ($4s^2S_{1/2}$, $3d^2D_{3/2,5/2}$, $4p^2P_{1/2,3/2}$) and a continuum. We take the level energy and oscillator strength values from NIST, the electron excitation coefficients from Melendez et al. (2007), and the collisional ionization coefficients are estimated using Seaton's formula (1964). The frequency scattering of spectral lines is considered within the framework of the Biberman – Holstein model (Biberman, 1947; Holstein, 1947, 1951). To calculate the probability escape, we use convolutions of Doppler and Holtsmark profiles for the hydrogen line and the Voigt profile for helium and calcium.

4 Calculation results

Table 2 shows the calculation results: the main parameters of the multicomponent layers whose calculated fluxes in spectral lines are close to the observed ones, whereas the deviation of the theoretical fluxes from the observed ones in the worst case is less than ten percent.

Table 2. Parameters of composite layers for each observation episode.

O	N, cm^{-3}	Δh, km	T_e, K	J, erg cm^{-2} s^{-1}
I	$2.5\,10^{12}$	50	9500	$1.5\,10^{3}$
	$1\,10^{16}$	350	5400	—
II	$2.0\,10^{12}$	120	14000	$5.0\,10^{3}$
	$4.3\,10^{12}$	50	6950	—
	$1\,10^{16}$	150	5500	—
III	$3.0\,10^{12}$	390	10000	$1.0\,10^{4}$
	$1.85\,10^{16}$	160	5600	—

The three observation episodes are separated from each other by horizontal lines. We take into account the vertical inhomogeneity of the luminous plasma by a set of elementary layers located one above the other with fixed values of gas temperature and density. To achieve the required accuracy of the theoretical simulation of observations, in the case of the first and third episodes, it turned out sufficient to apply a model of two elementary layers, and in the case of the second episode, three layers were required.

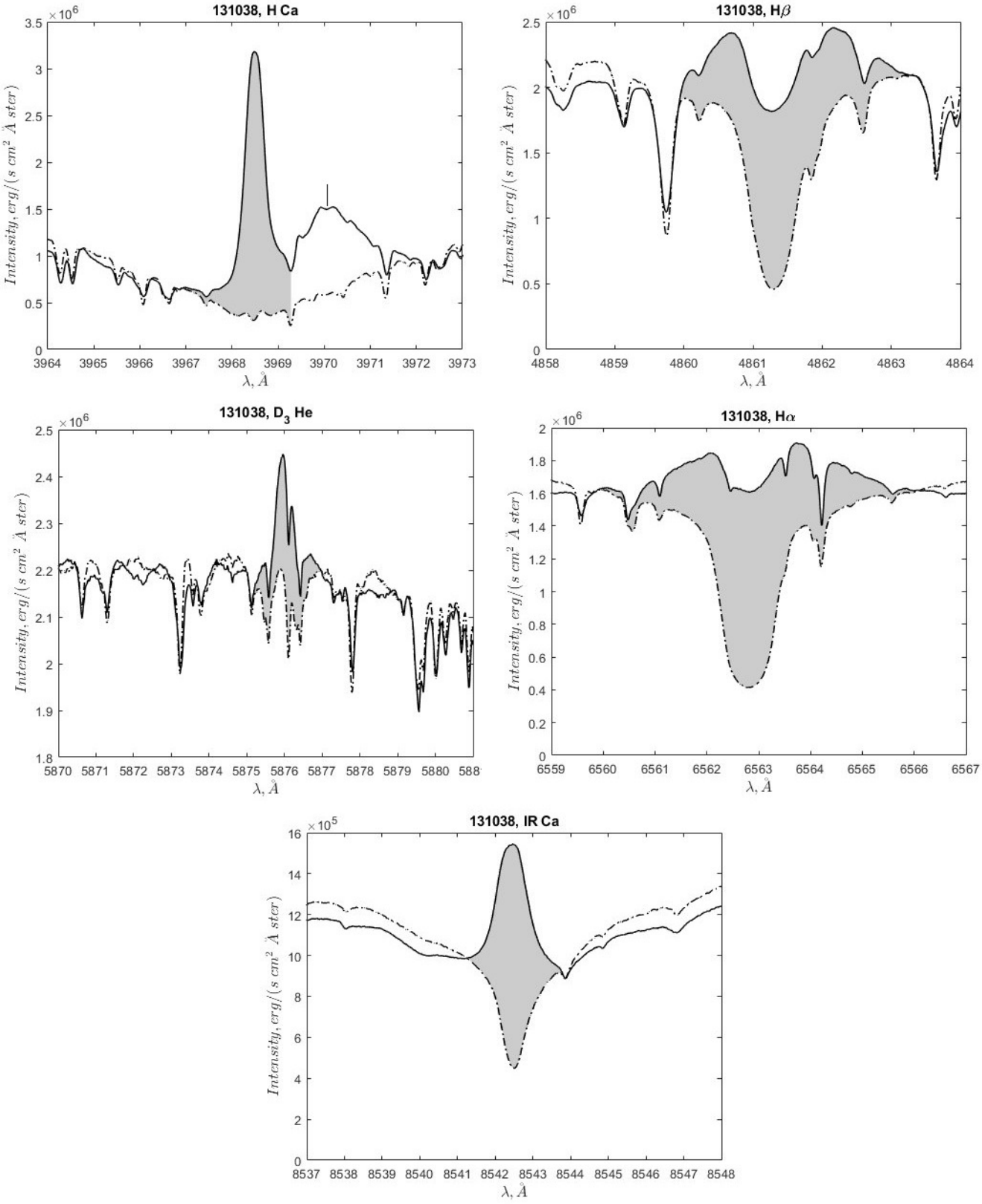

Fig. 3. Profiles of spectral lines (active and quiet chromosphere). The value marked in the H Ca II spectrum corresponds to the H_ϵ line.

The first column shows the episode number, and the rest show the parameters of the elementary layers: concentration N in 1/cm^3, layer thickness Δh in kilometers, gas temperature T_e in Kelvins, and the energy flux of suprathermal particles J in units of erg/cm^2/s. The order of the rows for each observation moment corresponds to the geometric arrangement of the corresponding physical layers, with the row immediately above the horizontal line containing information about the lowest layer.

Let us discuss the data in Table 2. First, they show the fundamental applicability of the proposed model to the available observations. Further, the need to introduce several theoretical layers with different parameters indicates the vertical inhomogeneity of the luminous gas.

Table 3. Ratio $R\alpha$ of fluxes in the Hα and H Ca II lines and the Balmer decrement δ.

O	I	II	III
$R\alpha$	1.0	1.6	1.3
δ	1.45	1.50	1.22

More detailed conclusions follow from the ratios of fluxes in spectral lines. Thus, the very low temperature value of the lower layer in the first episode follows from a relatively large flux of the calcium resonance line in relation to the hydrogen Hα line. Let us introduce the notation $R\alpha$ for the ratio of fluxes $F(\mathrm{H}\alpha)$ in the Hα lines and $F(R)$ in the H Ca II resonance line: $R\alpha = F(\mathrm{H}\alpha)/F(R)$. Its value for the three episodes is given in the second row of Table 3.

The calculated value of $R\alpha$ is close to unity at $T_e \approx$ 5400 K and increases with increasing temperature. The relatively small values of $R\alpha$ in the third and fourth columns of Table 3 indicate that the temperature of the lower layer remains low in subsequent episodes as well. Therefore, we assume, in accordance with Fig. 4 (images obtained using the Helioviewer program, Müller et al., 2017), that the flare occurred above the sunspot penumbra. According to new ideas (Rezaei, 2018), the umbra of sunspots consists of a relatively cold medium with inclusions of hotter elements. The most part is a cold medium with $T_e \sim 4000$ K. Hot inclusions occupy 5–10 % of the sunspot umbra area and $T_e \sim 5400$ K in them. Accordingly, in our calculations we took the blackbody temperature T_b equal to 5000 K.

The third row of Table 3 contains the Balmer decrement $\delta = F(\mathrm{H}\alpha)/F(\mathrm{H}\beta)$. Its low values indicate self-absorption in the Balmer series lines. Model calculations require at least two layers. In the lower warm dense layer, powerful radiation with a steep decrement is formed, and the upper rarefied hot layer smooths the decrement, more strongly absorbing radiation in the Hα line. We note that the hydrogen lines themselves can be explained in a simple model of a homogeneous layer, but this results in too low fluxes in the calcium lines.

Let us turn to the calcium lines. We introduce the notation r for the ratio of fluxes of the resonance and infrared lines, $r = F(3968)/F(8542)$. As calculations have shown, relatively small observed values of the ratio, $r < 2.5$, at a large flux in the resonance line, $F(3968) \approx 10^7$ erg/cm^2/s, indicate that the radiation in the calcium lines comes from a dense, weakly heated gas. In the case of r>1.7, it turned out possible to explain the observed fluxes within the framework of a homogeneous layer model. But the very shallow decrement in the second episode ($r = 1.4$) requires the assumption of two layers of different temperature and density to explain it. Although the theoretical decrement in them is greater than the observed one, the flattening of the decrement of the total radiation occurs due to partial absorption by the upper, more strongly heated and less dense layer. The optical depth in the resonance line $\lambda = 3968$ Å is almost an order of magnitude smaller than in the infrared transition $\lambda = 8542$ Å. As a result, the resonance line is attenuated to a greater extent than the infrared line. Therefore, two layers of calcium line formation were required to explain the second episode. Thus, the Ca II

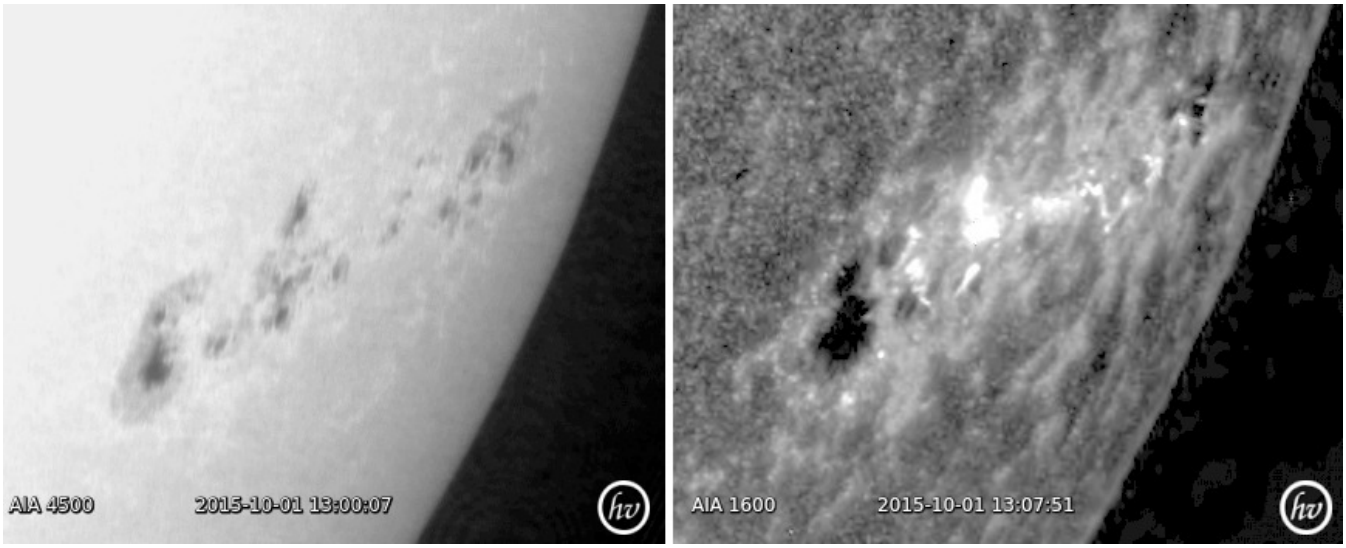

Fig. 4. Left image: NOAA 12422, SDO AIA 4500 07:00:07 UT. Right image: AIA 1600 13:07:51 UT.

ion lines originate from a dense, weakly heated region with possible absorption by upper hotter layers. The increase in fluxes in the resonance and infrared calcium lines over time indicates a gradual increase in the temperature of the lower layer.

Finally, about the role of suprathermal particles. They practically do not affect the radiation power in the hydrogen and calcium lines but play a significant role for the radiation in the helium line λ = 5876 Å. Calculations have shown that its enhancement is mainly due to an increase in the flux of suprathermal particles and only secondarily to an increase in temperature. The reason for this is the high excitation potential (23 eV) of the upper level of the D3 line λ = 5876 Å compared to the Hα line (12 eV) and H Ca II (3 eV). The heating of the coronal gas by suprathermal particles may entirely provide the observed increase in X-ray emission. For example, the flux in the range of 1–8 Å at the moment of maximum (Fig. 1), when recalculated to the surface of the Sun equal to $2.3\,10^3$ erg/cm^3/s, is obtained for a gas column with a height of 1000 km with a temperature of 10^8 K and an electron density of 10^9 cm^{-3}.

5 Conclusions

1. Observations of the emission lines of the 2015–10–01 flare can be explained in a model of the chromospheric gas heated from below by magnetohydrodynamic waves and ionized and excited from above by a flux of suprathermal particles.
2. Calcium lines are formed in deep dense and least heated layers, whereas radiation in hydrogen lines is dispersed in regions with different density and temperature.
3. The luminescence in the helium line λ = 5876 Å is largely due to suprathermal particles.
4. The large flux in the H Ca II line in the first episode, comparable to Hα, indicates that the flare occurred in the sunspot penumbra region, whose temperature does not exceed 5400 K. The subsequent decrease in the flux in the H Ca II line relative to Hα indicates a gradual heating of the lower layers of the gas.
5. The dynamics of the flare development shows the presence of a strong magnetic field that does not change during the flare. The contrast of the loop structure, which increases by the end of the flare, indicates an increase in the amount of matter in the magnetic structures and a decrease in its temperature. This creates inhomogeneities in the field of the flare structure.

The authors thank the GOES, SDO, and Ondřejov Observatory teams for the opportunity to conduct observations and use the data.

References

Abbett W.P., Hawley S.L., 1999. Astrophys. J., vol. 521, p. 906.
Allred J.C., Hawley S.L., Abbett W.P., Carlsson M., 2006. Astrophys. J., vol. 644, p. 484.
Belova O.M., Bychkov K.V., 2018. Astrofizika, vol. 61, no. 2, p. 255. (In Russ.)
Biberman L.M., 1947. ZhETF, vol. 17. p. 416. (In Russ.)
Bychkov K.V., Morchenko E.S., 2011. Vestnik Moskovskogo Universiteta. Fizika, no. 3, p. 89. (In Russ.)
Crespo-Chacón I., Montes D., Garcia-Alvarez D., et al., 2006. Astron. Astrophys., vol. 452, p. 987.
Grinin V.P., Katysheva N.A., 1980. Izv. Krymsk. Astrofiz. Observ., vol. 59, p. 66. (In Russ.)
Hawley S.L., Fisher G.H., 1992. Astrophys. J. Suppl. Ser., vol. 78, p. 565.
Holstein T., 1947. Phys. Rev., vol. 72, p. 1212.
Holstein T., 1951. Phys. Rev., vol. 83, p. 1159.
Houdebine E.R., 2003. Astron. Astrophys., vol. 397, p. 1019.
Johnson L.C., 1972. Astron. J., vol. 174, p. 227.
Kotrč P., 2009. Cent. Eur. Astrophys. Bull., vol. 33, p. 327.
Melendez M., Bautista M.A., Badnell N.R., 2007. Astron. Astrophys., vol. 469, p. 1203.
Müller D, Nicula B, Felix S., et al., 2017. Astron. Astrophys., vol. 606, p. A10
Rezaei R., 2018. Astron. Astrophys., vol. 609, p. A73.
Schmidt S.J., Kowalski A.F., Hawley S.L., et al., 2012. Astrophys. J., vol. 745, p. 14.
Seaton M.J., 1964. Planetary Space Sci., vol. 12, p. 55.